MOLECULAR AND CELLULAR BIOLOGY, Sept. 1987, p. 3277–3286
0270-7306/87/093277-10$02.00/0

Vol. 7, No. 9

Identification of a Complex Associated with Processing and Polyadenylation In Vitro of Herpes Simplex Virus Type 1 Thymidine Kinase Precursor RNA

FANG ZHANG AND CHARLES N. COLE*

Department of Biochemistry, Dartmouth Medical School, Hanover, New Hampshire 03756

Received 13 April 1987/Accepted 19 June 1987

Cleavage and polyadenylation of substrate RNAs containing the herpes simplex virus type 1 (HSV-1) thymidine kinase (*tk*) gene polyadenylation signal region were examined in a HeLa cell nuclear extract. 3′-End RNA processing was accurate and efficient and required ATP and Mg^{2+}. Cleavage, but not polyadenylation, occurred in the presence of EDTA or when ATP was replaced with 3′ dATP (cordycepin) or AMP(CH_2)PP, a nonhydrolyzable analog of ATP. Processing in vitro and in vivo showed the same signal element requirements: a series of substrates containing linker scanning, internal deletion, and small insertion mutations was processed with the same relative efficiencies and at the same sites in vitro and in vivo. A complex involved in 3′-end RNA processing was identified by gel mobility shift analysis. This complex formed rapidly, reached a maximum level after 20 to 30 min, and was much reduced after 2 h. Very little complex was formed at 0°C or with substrates lacking a polyadenylation signal. Entry of ^{32}P-labeled *tk* substrate into the complex could be prevented by addition of excess ^{35}S-labeled *tk* or adenovirus L3 precursor RNAs. Competition was not observed with *tk* RNAs lacking a complete polyadenylation signal.

In eucaryotic cells, mRNAs are formed from precursors through a series of processing steps which include 5′ capping, methylation, splicing, and 3′-end RNA processing (for reviews, see references 3, 26, and 34). Most mRNAs contain a tract of polyadenylic acid at their 3′ ends. Polyadenylation occurs at a site formed by endonucleolytic cleavage of the primary transcript (35, 36); approximately 200 adenylic acid residues are added at this cleavage point.

Two sequence elements are required for efficient cleavage and polyadenylation. Almost all polyadenylated mRNAs contain the hexanucleotide 5′-AAUAAA-3′, or a closely related variant, 6 to 30 bases upstream from the polyadenylation site (13, 39). A second essential signal element (GU or U rich) is located downstream of the cleavage site (9, 10, 16, 20, 27, 41, 47). The second element is less highly conserved than AAUAAA (28).

Cell-free systems have been developed in which precursor RNAs are accurately and efficiently processed and polyadenylated (30–32). Using a substrate containing the adenovirus L3 polyadenylation signal region, Moore and Sharp (32) demonstrated that both cleavage and polyadenylation require ATP but that ATP analogs could substitute for ATP in the cleavage reaction. In most studies, divalent cations and a 5′ cap structure were not required for processing. The in vitro and in vivo processing reactions require the same signals. Point mutations in AATAAA of both the simian virus 40 (SV40) early and late polyadenylation signals resulted in drastically reduced levels of cleavage and polyadenylation (1, 45). Substrates terminating between the two signal elements of either the adenovirus L3 or E2A polyadenylation signals were processed much less efficiently in vitro than substrates extending through the downstream element (21, 33). Although small nuclear ribonucleoprotein particles (snRNPs) are required for splicing and for formation of histone mRNA 3′ ends by endonucleolytic cleavage (for a review, see reference 3), a role for snRNPs in cleavage and polyadenylation remains uncertain (1, 4, 17, 22, 24, 25, 31, 32, 37, 40).

We described previously the detailed mutational analysis of the processing and polyadenylation signal region of the herpes simplex virus type 1 (HSV-1) thymidine kinase (*tk*) gene (8, 9, 47). The *tk* gene contains two copies of the AATAAA hexanucleotide and a GT cluster located from 20 to 38 bases downstream from the first AATAAA. The first AATAAA is essential for 3′-end RNA processing; deletion of this element, without alteration of the spacing of other sequences, abolished the production of poly(A)$^+$ *tk* mRNA. Replacement of the second AATAAA with a linker had little effect. When different portions of the GT cluster were replaced with a linker, the amount of *tk* mRNA processed in the normal region was reduced, but normal 3′-end RNA processing was never abolished.

Here, we describe experiments in which precursor RNAs containing the HSV-1 *tk* polyadenylation signal were processed in vitro in HeLa cell nuclear extracts. Precursor RNAs prepared from *tk* mutations showed patterns of 3′-end RNA processing in vitro that were qualitatively and quantitatively similar to those seen in vivo. A complex that appears to be involved in 3′-end RNA processing was detected by gel mobility shift analysis of in vitro polyadenylation reactions. Complex formation required a processing signal, ATP or an ATP analog, and incubation at 30°C. ^{35}S-labeled *tk* or adenovirus L3 pre-mRNAs were able to compete for complex formation with ^{32}P-labeled *tk* pre-mRNA. *tk* substrates lacking both AAUAAAs, the GU cluster, or the entire poly(A) signal region were unable to compete for complex formation or 3′-end RNA processing.

MATERIALS AND METHODS

Mutations and mutant constructions. pTK2R/SV010 and *tk* linker scanning, internal deletion, small insertion, and 3′ resection mutations have been previously described (9, 47). Templates for RNA precursors were prepared by ligating the *Sma*I-to-*Pst*I fragment of pTK2R/SV010 or various muta-

* Corresponding author.

tions with the large *Sma*I-to-*Pst*I fragment of pGEM1 (Promega Biotech, Madison, Wis.). The *Sma*I-to-*Pst*I fragment of pTK2R extends from 27 bp upstream of the *tk* termination codon to 500 bp downstream of the poly(A) sites. This fragment also contains a short polylinker and pBR322 sequences from 4363 to 3609. The Delta7Ca/*Dra*I plasmid, which produces an RNA containing the L3 polyadenylation signal region of adenovirus type 2, was kindly provided by J. R. Nevins (Rockefeller University, New York, N.Y.). All plasmids were propagated in *Escherichia coli* HB101. Established procedures were used for transfection of bacterial cells (29), analysis of plasmid DNAs in minilysates (2), and purification of plasmid DNAs (2, 7).

Analysis of *tk* RNA in vivo. Transfection of Cos-1 cells, preparation of cytoplasmic RNA, and S1 nuclease analysis have been described previously (47).

In vitro transcription. HeLa cell nuclear extracts were prepared as previously described (12), except that phenylmethylsulfonyl fluoride was omitted and 1.5 mM $MgCl_2$ was added to the final dialysis buffer.

Capped RNA precursors were synthesized in vitro by using T7 RNA polymerase (11). Transcription was performed at 37°C for 2 h in buffer containing 40 mM Tris chloride (pH 7.5), 6 mM $MgCl_2$, 2 mM spermidine, 10 mM NaCl, 0.5 mM each ATP and CTP, 0.3 mM GTP, 1.2 mM G(5')ppp(5')G (P-L Biochemicals, Inc., Milwaukee, Wis.), and 0.01 mM [^{32}P]UTP. To produce ^{35}S-labeled RNA, the same conditions were used, except that 0.5 mM [^{35}S]UTP was used. Full-length transcripts were eluted from a 5% polyacrylamide gel in TBE buffer (89 mM Tris hydroxide, 89 mM boric acid, 2.5 mM EDTA, pH 8.3) by soaking the crushed gel slice overnight in 10 mM Tris chloride (pH 8.0)–1 mM EDTA.

3'-end RNA processing reactions were performed at 30°C in 20 μl containing 6.4 μl of nuclear extract, 1 mM ATP, 20 mM creatine phosphate, 6.4 mM HEPES (*N*-2-hydroxyethylpiperazine-*N*'-2-ethanesulfonic acid; pH 7.9), 32 mM KCl, 0.5 mM $MgCl_2$, 0.06 mM EDTA, 0.2 mM dithiothreitol, 6.4% glycerol, and 3% polyvinyl alcohol. Certain reactions, as indicated in the text, received 1 mM cordycepin triphosphate (3' dATP; Sigma Chemical Co., St. Louis, Mo.), AMP(CH_2)PP (Pharmacia, Inc., Piscataway, N.J.) or AMPP(CH_2)P (Pharmacia) in place of ATP. Except where indicated, precursor RNA was present at a concentration of 0.25 to 0.50 nM. The reaction was stopped by addition of 10 volumes of 50 mM Tris chloride (pH 8.0)–10 mM EDTA–10 mM NaCl. RNA was extracted once with phenol-chloroform-isoamyl alcohol (50:50:1) and once with chloroform-isoamyl alcohol (50:1) and ethanol precipitated.

After the reactions, RNAs were analyzed by electrophoresis on 5% denaturing acrylamide–7 M urea gels. For S1 nuclease analysis, unlabeled probes were prepared by *Sma*I or *Bst*NI cleavage of plasmids used as templates to prepare substrate RNAs. S1 analysis was performed as described previously (47).

Gel mobility shift analysis. Conditions similar to those used to study RNA splicing by gel mobility shift analysis were used (23). Unless indicated, 3'-end RNA processing reactions were incubated at 30°C for 30 min in a 10-μl reaction volume. Reactions were stopped by addition of heparin to 5 mg/ml and incubation for an additional 10 min at 30°C. Electrophoresis was carried out in a 4% acrylamide gel (25 cm long, 0.7 mm thick; acrylamide-*N*,*N*'-methylene bisacrylamide ratio, 80:1) in either 0.5× TBE buffer [89 mM Tris(hydroxymethyl)aminomethane, 89 mM boric acid, 2.5 mM EDTA, pH 8.3] or TG buffer (50 mM Tris glycine, pH 8.8) at 350 V until the xylene cyanol dye had migrated 15 cm. Electrophoresis was conducted in a cold room. Gels were dried and subjected to autoradiography with Kodak XAR-5 film at −70°C.

Two-dimensional gel analysis of the products of in vitro 3'-end RNA processing. Samples were prepared and subjected to electrophoresis as described above for gel mobility shift analysis. The entire gel lane was excised and inserted into a single wide horizontal well of a denaturing 5% acrylamide–7 M urea gel (15 cm long, 1.5 mm thick) and subjected to electrophoresis at 300 to 400 V until the bromphenol blue dye had migrated to the bottom of the gel. The gel was dried and subjected to autoradiography with Kodak XAR-5 film at −70°C.

Competition experiments. Competitor RNAs were transcribed by T7 or SP6 RNA polymerases and labeled with [^{35}S]UTP to permit determination of RNA concentrations. Competitors were added at various concentrations to in vitro RNA processing reaction mixtures containing ^{32}P-labeled substrate RNA. In general, competitors were present at 5- to 300-fold molar excess over the concentration of ^{32}P-labeled substrate RNA. The following competitor RNAs were used: (i) TK, RNA containing the complete *tk* polyadenylation signal region and having the same structure as *tk* substrate RNA; (ii) adenovirus L3, RNA containing the adenovirus L3 polyadenylation signal region and having the same structure as adenovirus L3 substrate RNA; (iii) 3'-TK-DL(−21/49), an internal deletion mutation lacking all *tk* polyadenylation signal elements (47) (competitor RNA was produced from a pGEM1 clone containing the *Sma*I-*Pst*I fragments of this mutation after digestion of the clone with *Hae*III and transcription with T7 RNA polymerase); (iv) TK/GU, a competitor containing sequences from phage T7, plus the complete GU cluster of the HSV-1 *tk* gene and downstream sequences, and lacking both AAUAAAs; (v) 315, a competitor derived from pTK315/SV010 (9) and containing phage T7 sequences and *tk* sequences extending only as far as the two AATAAAs.

RESULTS

In vitro processing of pre-mRNA substrates containing the polyadenylation signal region of the HSV-1 *tk* gene. Our previous studies defined the signals for *tk* mRNA cleavage and polyadenylation in vivo in Cos-1 cells (9, 47). To study *tk* 3'-end RNA processing in vitro in HeLa cell nuclear extracts, we inserted the *Sma*I-*Pst*I fragment of pTK2R/SV010, containing the polyadenylation signal (Fig. 1) into *Sma*I-*Pst*I-digested pGEM1, yielding pT7/TK (Fig. 1B). The *Sma*I site is located 27 bases upstream of the *tk* protein synthesis termination codon and 75 bases upstream of the first of two AATAAAs found in the *tk* gene. This fragment contains the complete 3' untranslated region of *tk* mRNA, both AATAAAs, the downstream GT cluster, and approximately 500 bp of additional HSV-1 DNA. When pT7/TK was digested with *Bst*NI and transcribed by using T7 RNA polymerase, a 160-nucleotide RNA was produced (Fig. 1C).

tk mRNA is polyadenylated in vivo at multiple sites (47). The major site (Fig. 1C, thick arrow) is located between the two AAUAAAs. (A prominent minor site [thin arrow] is located downstream of the distal AAUAAA and just upstream of the GU cluster.) Thus, the major products of correct endonucleolytic processing of this pre-mRNA in vitro should be a 55-nucleotide 3' half molecule and a polyadenylated 105-nucleotide 5' half molecule. The site of cleavage can be mapped precisely by S1 nuclease analysis.

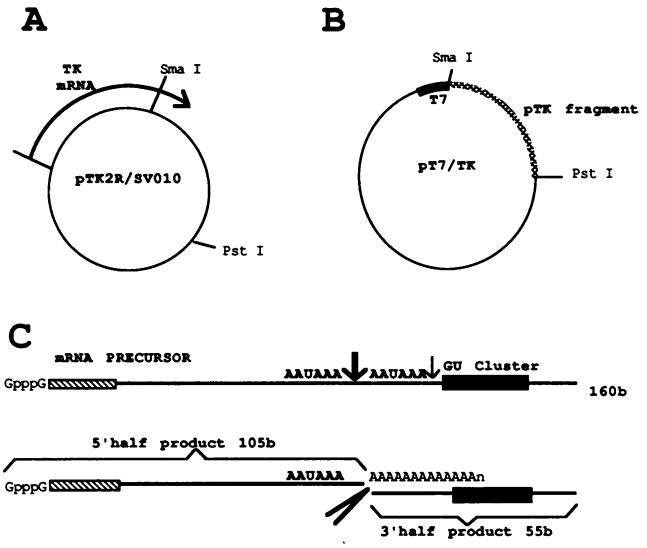

FIG. 1. (A) Plasmid pTK2R/SV010. This plasmid contains the HSV-1 *tk* gene flanked by the SV40 origin of replication upstream and a polylinker sequence downstream. The HSV-1 DNA in pTK2R/SV010 includes the complete *tk* gene, including sequences extending upstream through the promoter to the next *Pvu*II site and sequences extending 552 bp downstream beyond the polyadenylation site. (B) Plasmid pTK/T7. The *Sma*I-*Pst*I fragment of pTK2R/SV010, containing the complete polyadenylation signal region, was ligated with the large *Pst*I-*Sma*I fragment of pGEM1. (C) Diagram of precursor and products of in vitro polyadenylation of HSV-1 *tk* precursor RNA. The capped, 160-nucleotide precursor was prepared by transcription of *Bst*NI-digested pTK/T7 with T7 RNA polymerase. The hatched box shows the position of the pGEM1 sequence in the precursor. The solid box indicates the GU cluster. The major cleavage site is indicated by a thick arrow downstream of the first AAUAAA; the thin arrow indicates the position of a prominent minor cleavage site. Endonucleolytic cleavage at the major site produces a 105-nucleotide 5′ half molecule and a 55-nucleotide 3′ half molecule, indicated by the bracket. An average of 250 residues was added to the 5′ half molecule during processing. b, Base.

When unlabeled DNA probe, cleaved at the *Sma*I site, was annealed with ^{32}P-labeled RNA isolated by phenol extraction after in vitro RNA processing, the probe protected the last 76 bases of the 5′-RNA half molecules from S1 digestion (Fig. 2B); it also protected a 134-base portion of substrate.

Capped T7/TK RNA was incubated in HeLa cell nuclear extract in the presence of ATP, creatine phosphate, Mg^{2+}, and various concentrations of EDTA. Samples were isolated after 1 or 2 h and analyzed by electrophoresis on a denaturing acrylamide-urea gel (Fig. 2A). Input substrate is shown in Fig. 2, lane 1. The 3′ half molecule was prominent after 1 h of incubation (lane 2) but could not be detected after 2 h of incubation. After 2 h (lane 3), approximately 60% of the T7/TK precursor RNA migrated more slowly than substrate and had been polyadenylated [based on oligo(dT)-cellulose chromatography (data not shown)]. S1 nuclease analysis was performed on oligo(dT)-selected RNA; after 2 h of incubation (Fig. 2B), approximately 55% of the poly(A)$^+$ *tk* RNA had been cleaved at the normal processing site and 45% was uncleaved polyadenylated substrate. Thus, *tk* precursor RNA was processed accurately and with efficiency comparable to that observed with various other 3′-end RNA processing substrates. When a *tk* pre-mRNA substrate lacking a polyadenylation signal was used, there was no cleavage (Fig. 2A, lane 13) and less than 5% of the substrate became polyadenylated at its 3′ end during a 2-h incubation period (data not shown).

Addition of EDTA to the reaction inhibited polyadenylation but not cleavage and also inhibited degradation of the 3′ half molecules. Partial inhibition of polyadenylation was seen with 0.6 mM (Fig. 2A, lanes 4 and 5) or 1.0 mM (Fig. 2A, lanes 6 and 7) EDTA; inhibition was complete at 2.0 mM (Fig. 2A, lanes 8 and 9) or 3.0 mM (Fig. 2A, lanes 10 and 11) EDTA. These results agree with those described by others using other polyadenylation signals (32, 45). In the presence of Mn^{2+}, longer poly(A) tails (approximately 400 to 600 bases) were added and a larger fraction of uncleaved molecules was polyadenylated (data not shown). All subsequent experiments were performed in the presence of 0.5 mM Mg^{2+}.

Experiments in which substrate concentration ranged from 0.5 to 45 nM indicated that the amount of cleavage and polyadenylation increased linearly with substrate concentration in the 0.5 to 5.0 nM range (data not shown). Above this, the amount of polyadenylation increased more slowly and

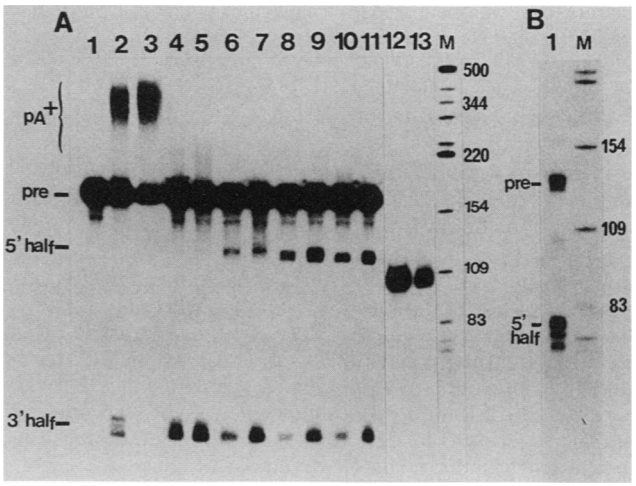

FIG. 2. In vitro processing and polyadenylation of *tk* precursor RNA. (A) RNA precursor was incubated in the presence of Mg^{2+} or various concentrations of EDTA. The reaction mixtures were phenol extracted and analyzed by electrophoresis on a 5% acrylamide–7 M urea gel. The substrate for lanes 1 to 11 was T7/TK RNA containing the wild-type 3′-end RNA processing signal. The substrate for lanes 12 and 13 was derived from mutant 3′TK-DL(−21/49; reference 47) and lacks the AAUAAAs and the GU cluster. Lanes: 1 to 3, no EDTA; 4 and 5, 0.5 mM EDTA; 6 and 7, 1.0 mM EDTA; 8 and 9, 2.0 mM EDTA; 10 and 11, 3.0 mM EDTA; 12 and 13, no EDTA. Substrate was incubated under standard processing conditions (see Materials and Methods) for 0 min (lanes 1 and 12), 1 h (lanes 2, 4, 6, 8, and 10), or 2 h (lanes 3, 5, 7, 9, 11, and 13). (B) S1 nuclease protection analysis of the products of in vitro polyadenylation of *tk* precursor RNA. The precursor was incubated under processing conditions for 2 h. The reaction mixtures were phenol extracted and subjected to oligo(dT)-cellulose chromatography. The poly(A)$^+$ fraction (pA$^+$) was analyzed by S1 nuclease mapping with *Sma*I-digested pTK2R/SV010 as the probe. After hybridization and S1 nuclease digestion, the protected RNA fragments were analyzed by electrophoresis on a 5% polyacrylamide–7 M urea gel. The band marked 5′ half represents cleaved and polyadenylated substrate. The band marked pre corresponds to precursor polyadenylated at its 3′ end without cleavage. The numbers alongside the lanes containing markers (M) indicate molecular size in nucleotides.

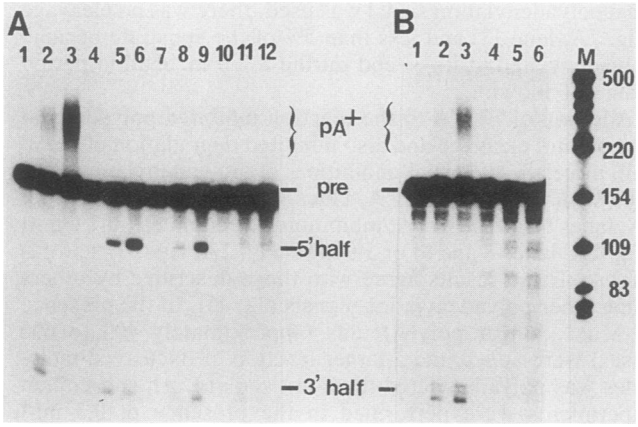

FIG. 3. (A) In vitro processing and polyadenylation in the presence of ATP analogs. Substrate T7/TK RNA was incubated under processing conditions, containing ATP (lanes 1 to 3), 3′ dATP (cordycepin) (lanes 4 to 6), AMP(CH_2)PP (lanes 7 to 9), or AMPP(CH_2)P (lanes 10 to 12). Reactions were stopped after 0 h (lanes 1, 4, 7, and 10), 1 h (lanes 2, 5, 8, and 11), or 2 h (lanes 3, 6, 9, and 12). (B) In vitro processing and polyadenylation in the presence (lanes 1 to 3) or absence (lanes 4 to 6) of ATP. T7/TK substrate RNA was incubated for 0 min (lanes 1 and 4), 30 min (lanes 2 and 5), or 1 h (lanes 3 and 6). After phenol extraction, RNAs were analyzed on 5% polyacrylamide–7 M urea gels. The numbers alongside the lanes containing markers (M) indicate molecular size in nucleotides.

the proportion of uncleaved substrate in the poly(A)$^+$ fraction increased slightly. In subsequent experiments, substrate concentrations below 2 nM were used, except where noted.

The effects of ATP analogs on 3′-end processing are shown in Fig. 3A. Polyadenylation, but not cleavage, was prevented by 3′-ATP (lanes 4 to 6) and AMP(CH_2)PP (lanes 7 to 9). In the presence of AMPP(CH_2)P, less substrate was processed and the poly(A) tails were shorter (lanes 10 to 12) than in the presence of ATP (Fig. 3A and B, lanes 1 to 3). There was little or no processing when ATP was omitted from the reaction (Fig. 3B, lanes 4 to 6), but an increase in substrate degradation was observed.

In vitro 3′-end RNA processing of *tk* RNA substrates containing linker scanning, internal deletion, and small insertion mutations. We described previously (47) in vivo 3′ RNA processing of a series of linker scanning, internal deletion, and small insertion mutations. The structure of the poly(A) signal regions of these mutations is shown schematically in Fig. 4A. In vivo, these mutations show reproducible qualitative (Fig. 4C; reference 47) and quantitative (47) alterations in 3′-end RNA processing. Substrate RNAs were incubated for 2 h in a standard reaction mixture, and the pattern of 3′-end RNA processing was analyzed by S1 nuclease mapping. All RNAs were annealed with homologous probes. Comparison of corresponding lanes in Fig. 4B and C indicated that 3′-end RNA processing occurs at the same sites in vitro and in vivo.

Since all RNA substrates used in vitro had approximately the same specific radioactivity, the relative efficiency of processing in vitro can be assessed by comparing the intensities of the S1-protected processed fragments (Fig. 4B). However, the ^{32}P-labeled probes used for analysis of RNA produced in vivo (Fig. 4C) had different specific activities. Relative processing efficiencies of these mutations in vivo were determined previously by annealing all RNAs to the same probe (47) and are listed in Fig. 4A. These in vivo

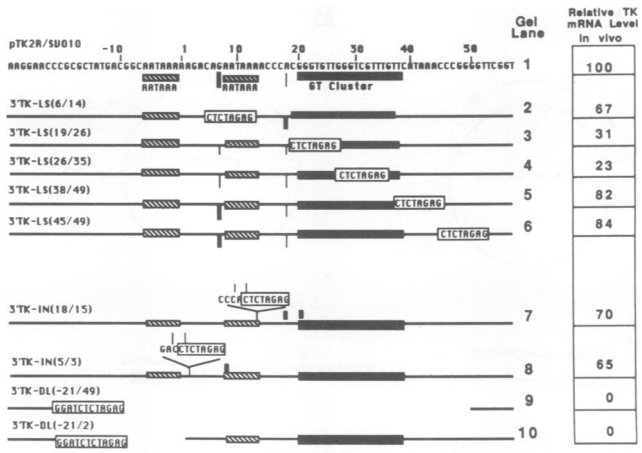

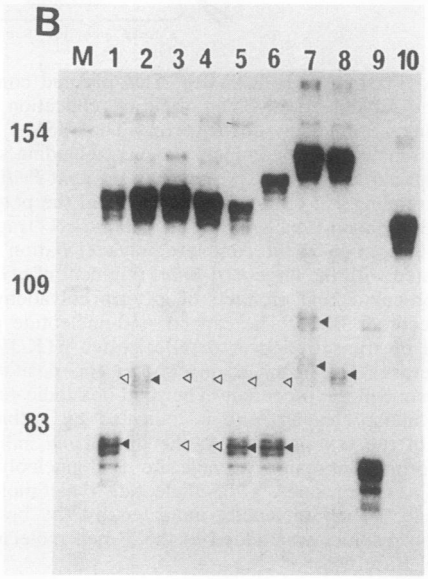

FIG. 4. Comparison of 3′-end processing of linker scanning, internal deletion, and small insertion mutations in vitro and in vivo. (A) Diagram of the polyadenylation regions of the mutations analyzed. In all cases, position +1 is defined as the first residue 3′ to the first copy of the AATAAA hexanucleotide. The two AATAAAs and the GT cluster sequences are underlined, and the linker sequence is boxed. Major and minor cleavage sites are indicated with thick and thin bars, respectively. The relative efficiencies of processing in vivo were determined previously (47). (B) S1 nuclease analysis of in vitro processing products from the wild type (T7/TK) and various mutant RNAs. In all cases, 3×10^4 dpm of ^{32}P-labeled substrate RNAs were used. All incubations were for 2 h. The reaction products were

efficiencies are approximately the same as efficiencies of processing in vitro (Fig. 4B).

The kinetics of in vitro 3'-end RNA processing of various mutant substrates were also examined. Substrates were incubated and analyzed as for Fig. 4B. Processing of wild-type substrate (T7/TK) was complete after 1 h of incubation (Fig. 5A, lane 4); at that time, approximately 55% of the input substrate had been processed. Processing of mutations 3'TK-LS(6/14) (Fig. 5B) and 3'TK-LS(38/49) (Fig. 5D) continued to increase throughout 5 h of incubation; at that time, the fraction of substrate processed was approximately 45%. Thus, these substrates were processed slightly less efficiently and less rapidly than the wild type. In vivo, these mutations were processed with slightly reduced efficiency (67 and 82% of the wild-type level, respectively). Processing of 3'TK-LS(26/35) (Fig. 5C) reached a plateau between 3 and 5 h of incubation. At that time, only a very small fraction of substrate had been cleaved. In vivo, this mutation produces only 23% as much *tk* mRNA as does the wild type (47). Of the various substrates tested, the wild-type *tk* substrate was processed most rapidly and efficiently.

Gel retardation analysis of a complex involved in 3'-end RNA processing. Factors and complexes involved in cleavage and polyadenylation have not been identified. For RNA splicing, an active complex called a spliceosome (5, 14, 18, 38) has been identified by glycerol gradient analysis and shown to contain snRNPs and other components. In other experiments (23), pre-mRNA substrates containing introns were incubated under splicing conditions with HeLa cell nuclear extracts; after a brief time, heparin was added to the reaction and the reaction mixture was analyzed on low-percentage, low-ionic-strength acrylamide gels. The mobility of the pre-mRNA was retarded substantially because of the association of substrate with the spliceosome. Similar gel retardation analyses have been useful in demonstrating the association of sequence elements within promoters and enhancers with protein factors (6, 15, 42, 43).

When precursor RNA containing the *tk* polyadenylation signal region was incubated with nuclear extract under polyadenylation conditions, substrate formed a complex that caused it to migrate substantially more slowly in low-percentage, low-ionic-strength acrylamide gels (Fig. 6). The free substrate is shown in Fig. 6A, lane 0. When mixed on ice with nuclear extract, all of the substrate migrated with reduced mobility (lane 1). A similar mobility shift was seen when any labeled RNA was mixed with nuclear extract and probably represents ribonucleoprotein (RNP). A further reduction in mobility was seen only under conditions associated with 3'-end RNA processing.

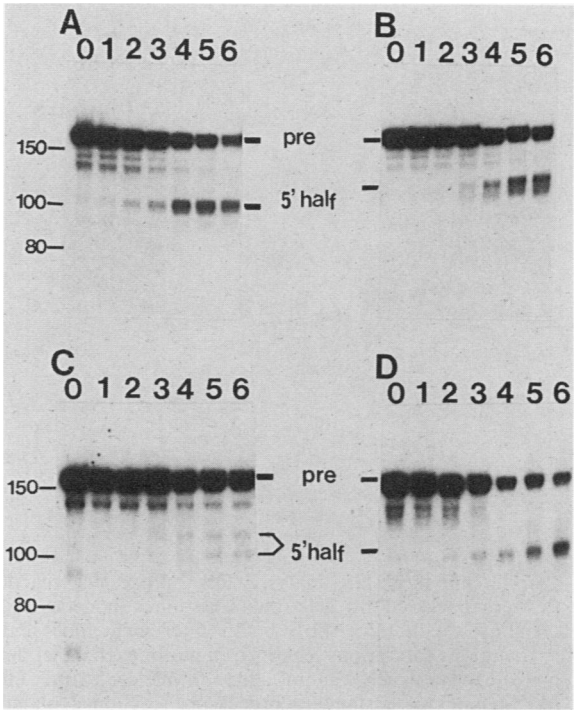

FIG. 5. Time course of processing of wild-type and mutant *tk* RNAs. Panels: A, wild-type substrate; B, 3'TK-LS(6/14); C, 3'TK-LS(26/35); D, 3'TK-LS(38/49). Samples were removed from processing reactions after 0 min (lanes 0), 15 min (lanes 1), 30 min (lanes 2), 1 h (lanes 3), 2 h (lanes 4), 3 h (lane 5), or 5 h (lanes 6), extracted with phenol, and analyzed by S1 nuclease mapping with homologous probes prepared by digesting each plasmid with *Bst*NI. Lanes 0 contain substrate RNAs not added to the processing reaction mixture. Samples were analyzed on a 5% polyacrylamide–7 M urea gel. The numbers to the left of panels A and C indicate molecular size in nucleotides.

When the reaction mixture was incubated at 30°C, a complex appeared rapidly and was almost gone within 2 h of incubation (lane 5), at a time when 3'-end RNA processing had ceased. Complex formation was stimulated by addition of ATP (compare lanes 6 and 7). A polyadenylation signal was also required. No complex formed with a substrate lacking the *tk* polyadenylation signal region (Fig. 6B, lanes 1 to 3). Incubation at 30°C was also necessary for complex formation; incubation at 0°C for 15 min did not result in a similar mobility shift (compare Fig. 6C, lanes 2 and 3).

A complex appeared without a lag period (Fig. 6D). In contrast, spliceosome assembly proceeds with a considerable lag (5, 18). This suggests that the polyadenylation complex is preformed since assembly is rapid and complexes migrating at intermediate positions were not seen.

During in vitro processing, the complex appeared transiently. As the amount of complex decreased, labeled material appeared which migrated between the positions of the complex and RNP (Fig. 6A, lanes 4 and 5, and D, lanes 5 to 7). To determine where the products and intermediates in processing migrated in this gel, a two-dimensional gel electrophoresis system was used (Fig. 7). Substrate was incubated under processing conditions for 30 min, mixed with heparin, and subjected to electrophoresis in two parallel gel lanes under the same conditions used for Fig. 6. One lane was dried and autoradiographed and appears horizontally at the top of Fig. 7B. The other was laid on top of a denaturing

phenol extracted and analyzed by S1 mapping. Unlabeled DNA probes were prepared by *Sma*I digestion of the plasmid used as a template for preparation of substrate RNAs. Protected RNA fragments were analyzed by electrophoresis on a 5% polyacrylamide–7 M urea gel. The arrowheads indicate the RNA products cleaved at the major processing site. The major unmarked band in each lane corresponds to unprocessed precursor RNAs. (C) S1 nuclease analysis of *tk* RNA produced in Cos-1 monkey kidney cells transfected by the mutations analyzed for panel B. Cytoplasmic RNA was isolated from Cos-1 cells 48 h after transfection (47). To prepare homologous probes, each plasmid was digested with *Bss*HII (position −89) and 3'-end labeled by using the Klenow fragment of DNA polymerase I. The *Bss*HII site is 12 bp upstream from the *Sma*I site. Protected probe fragments were analyzed in a 5% polyacrylamide–7 M urea gel. The numbers to the left and right of panels B and C, respectively, indicate molecular size in nucleotides.

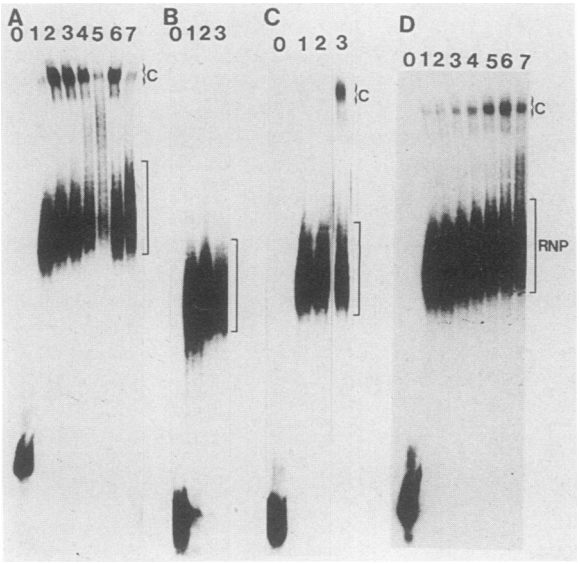

FIG. 6. Gel mobility shift analysis. RNA processing reaction mixtures were analyzed by electrophoresis on a nondenaturing polyacrylamide gel in 0.5× TBE buffer after incubation under different conditions for various lengths of time. In each panel, lane 0 contains substrate which was not added to nuclear extract mixtures. (A) Samples of a standard processing reaction containing wild-type T7/TK substrate were removed after 0 min (lane 1), 15 min (lane 2), 30 min (lanes 3 and 6), 1 h (lane 4), and 2 h (lane 5). The processing reaction was stopped by addition of heparin to 5 mg/ml, and incubation was continued for an additional 10 min at 30°C. In lane 7, ATP was omitted from the processing reaction, and incubation was for 30 min. (B) Processing reaction with a substrate [3′TK-DL(−21/49)] lacking the poly(A) signal region. Processing was stopped after 0 min (lane 1), 30 min (lane 2), and 2 h (lane 3). See Fig. 4A for the structure of this mutation, which lacks the polyadenylation signal elements. (C) Wild-type T7/TK substrate was incubated under processing conditions for 0 min (lane 1) or 15 min at either 0°C (lane 2) or 30°C (lane 3). (D) The processing reaction of T7/TK substrate was stopped after 0 min (lane 1), 2 min (lane 2), 5 min (lane 3), 10 min (lane 4), 15 min (lane 5), 30 min (lane 6), or 1 h (lane 7). The positions of the complex (C) and RNP are indicated.

polyacrylamide-urea gel, and material was electrophoresed into the second gel. Unprocessed substrate was found associated with the complex and in the RNP region of the first gel. Labeled material which migrated between RNP and the complex migrated more slowly than the substrate under denaturing conditions and comigrated with poly(A)$^+$ RNA isolated by oligo(dT)-cellulose chromatography (unpublished data). Free 3′ half molecules were not seen in this analysis. Perhaps cleavage occurs in the complex and half molecules are then released. Alternatively, heparin treatment may strip half molecules from the complex. In either case, once separated from the complex, the free 3′ half molecules would have migrated so rapidly that they would have been lost from the first-dimension gel. Figure 7A shows the pattern seen when the processing reaction was analyzed on a denaturing polyacrylamide-urea gel.

Processing complexes formed in the presence of ATP analogs were also examined by gel retardation analysis (Fig. 8). Under standard conditions with ATP, a complex could be seen (lane 2) and the amount was decreased substantially after 2 h of incubation (lane 3). In the absence of added ATP and in the presence of 3′ dATP (cordycepin triphosphate), AMP(CH_2)PP, or AMPP(CH_2)P, the amount of complex formed equaled or exceeded that seen with ATP (compare lanes 5, 8, and 11 with lane 2), and much remained after 2 h of incubation (lanes 6, 9, and 12). We conclude that analogs of ATP can substitute for ATP for complex formation.

The specificity of complex formation was examined by adding increasing amounts of ^{35}S-labeled competitor RNAs to reaction mixtures containing a constant amount of ^{32}P-labeled wild-type substrate (Fig. 9). All samples contained 10 fmol (0.5 nM) of labeled *tk* substrate. The left lane of each panel (marked INPUT) contained complexes formed by a mixture of substrate and extract without incubation at 30°C. After 30 min of incubation in the absence of competitor (lanes marked 0), a retarded complex (marked C) could be seen. Competitors were added at 5-, 50-, and 300-fold molar excess. ^{32}P-labeled substrate did not enter a complex in the presence of excess homologous *tk* substrate (T7/TK) or heterologous adenovirus L3 substrate (L3). Under these conditions, processing of ^{32}P-labeled substrate did not occur (data not shown).

No competition was seen with *tk* RNA lacking the poly(A) signal region [DL(−21/49)]. RNA substrates lacking the *tk* AAUAAAs (T7/GU) or the *tk* GU cluster (315) did not compete. The presence of these ineffective competitors had no effect on processing of the ^{32}P-labeled substrate (data not shown).

The ability of these competitor RNAs to form complexes themselves was also investigated. We found that a complex formed with wild-type *tk* substrate and adenovirus L3 substrate (Fig. 10, lane 4) but not with the other *tk* substrates.

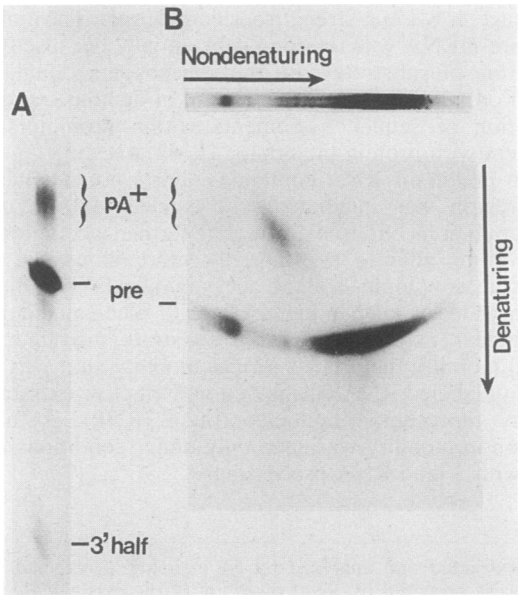

FIG. 7. Two-dimensional gel analysis of processing complexes. T7/TK substrate was incubated under standard processing conditions for 30 min at 30°C. (A) A sample of the reaction mixture was phenol extracted and electrophoresed in a denaturing 5% polyacrylamide–7 M urea gel in 0.5× TBE buffer and served as a marker for the second dimension of electrophoresis. (B) The remainder of the sample was mixed with heparin and subjected to electrophoresis in two parallel lanes of a 4% nondenaturing gel under the same conditions used for Fig. 6. One lane was dried and autoradiographed and is shown horizontally at the top of the panel. The other lane was laid on top of a denaturing 5% polyacrylamide–7 M urea gel. After electrophoresis, the gel was dried and autoradiographed. The positions of precursor (pre) and polyadenylated (pA$^+$) products are indicated.

DISCUSSION

In vitro 3′-end RNA processing of RNAs containing the HSV-1 *tk* polyadenylation signal region. In the experiments reported above, we described in vitro 3′-end RNA processing of precursor RNAs containing the HSV-1 *tk* polyadenylation signal. We found that precursor RNA was processed accurately and efficiently. The cleavage reaction required ATP or an analog of ATP [3′ dATP, AMP(CH_2)PP, or AMPP(CH_2)P] and occurred with similar efficiency in the presence or absence of Mg^{2+}. In the absence of Mg^{2+}, or when 3′ dATP or AMP(CH_2)PP replaced ATP, cleavage occurred with normal efficiency but polyadenylation was inhibited. Under these conditions, both the 5′ and 3′ half molecules were detected. When ATP was replaced with AMPP(CH_2)P, short poly(A) tails were added and the 3′ half molecules were less stable than when the other ATP analogs were present. The 3′ half molecules could also be detected in the presence of ATP and Mg^{2+} but were much less stable under these conditions, with no 3′ half molecules remaining after 2 h of incubation in the extract. These data indicate that processing of HSV-1 *tk* precursor RNA occurs through an endonucleolytic cleavage and has the same requirements for ATP and Mg^{2+} as reported by others (21, 32, 40, 44, 46).

In the presence of both ATP and Mg^{2+}, the 3′ half molecules appeared as a doublet (Fig. 1, lane 2; Fig. 3, lane 2; Fig. 8A); under all other conditions, only the shorter of the two species was detected. We do not understand the basis for this observation.

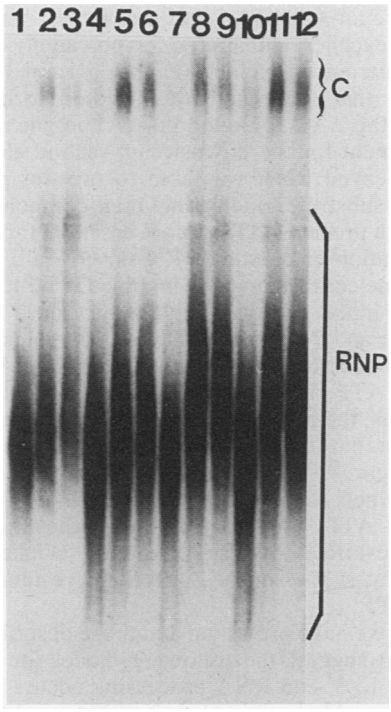

FIG. 8. Gel mobility shift analysis of processing complexes formed in the presence of ATP analogs. T7/TK RNA was incubated under processing conditions (containing ATP) (lanes 1 to 3) or under the same conditions but with ATP replaced by 3′ dATP (cordycepin) (lanes 4 to 6), AMP(CH_2)PP (lanes 7 to 9), or AMPP(CH_2)P (lanes 10 to 12). Reactions were stopped after 0 h (lanes 1, 4, 7, and 10), 1 h (lanes 2, 5, 8, and 11), or 2 h (lanes 3, 6, 9, and 12) and mixed with heparin, as described in the legend to Fig. 6. These samples were the same as those in Fig. 3A. The positions of the complex (C) and RNP are indicated.

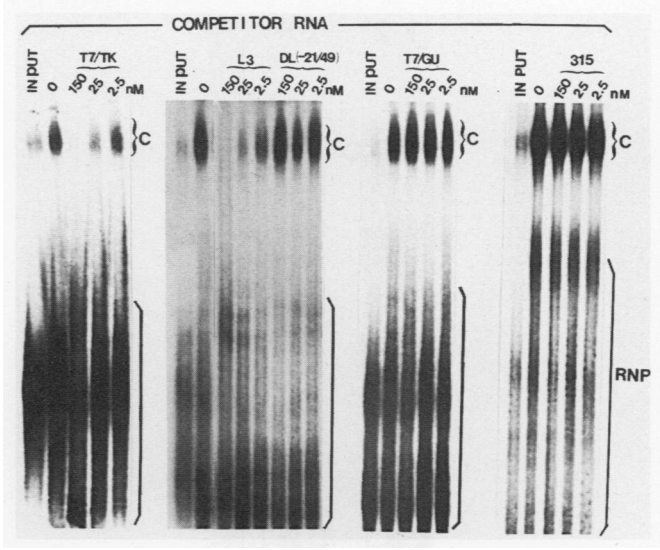

FIG. 9. Analysis of the ability of various RNAs to prevent complex (C) formation by T7/TK substrate. ^{32}P-labeled T7/TK RNA (0.5 nM) was incubated under processing conditions for 30 min in the absence of any competitor RNA (lanes 0) or in the presence of the indicated concentrations of ^{35}S-labeled competitors. Only the ^{32}P-labeled RNA was detectable under the autoradiography conditions used. In each set of three reactions containing competitor substrates, competitor was present in 300-, 50-, and 5-fold molar excess (left to right). Reactions were stopped by addition of heparin. Complexes were analyzed by electrophoresis on a nondenaturing 4% polyacrylamide gel containing 0.5× TBE buffer. All samples (except lanes 1) were incubated under processing conditions for 30 min. The lanes marked INPUT show the ^{32}P-labeled T7/TK substrate after addition to extract but without incubation at 30°C.

We described previously the patterns in vivo of 3′-end processing of a series of linker scanning, internal deletion, and small insertion mutations of the HSV-1 *tk* polyadenylation signal region (47). In vivo, these mutations cause reproducible shifts both in the sites of 3′-end formation and in the amounts of *tk* mRNA produced. In vitro, precursor RNAs carrying these mutations were processed at the same sites as in vivo and with the same relative efficiency. This extends the observation of others (21, 33) that efficient 3′-end RNA processing in vitro requires downstream sequences in addition to AAUAAA. The precise processing site(s) and the overall efficiency of cleavage and polyadenylation in vivo are determined, to a major extent, by the sequence of the polyadenylation signal region. Our finding that patterns of 3′-end RNA processing are both qualitatively and quantitatively very similar in vitro and in vivo indicates that in vitro processing reactions containing HeLa cell nuclear extract occur with great accuracy, respond to sequences very close to the cleavage site, and retain the same sensitivity to subtle mutational alterations as they do in intact cells.

Identification of a complex involved in 3′-end RNA processing. Using gel mobility shift analysis, we identified complexes between components of the HeLa cell nuclear extract and *tk* precursor RNA. All T7 RNA polymerase transcripts tested associated with extract components to form a complex, probably RNP, which migrated more slowly than free substrate on nondenaturing, low-ionic-strength acrylamide

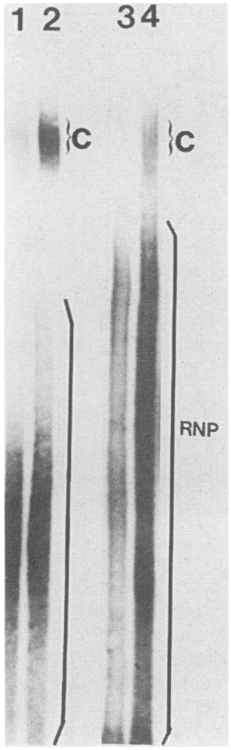

FIG. 10. Gel mobility shift analysis of the processing reaction containing adenovirus L3 substrate. Processing reactions containing T7/TK (lanes 1 and 2) or adenovirus L3 (lanes 3 and 4) RNA were stopped by addition of heparin after 0 min (lanes 1 and 3) or 30 min (lanes 2 and 4) of incubation. After further incubation for 10 min, products were analyzed by electrophoresis on a 4% nondenaturing polyacrylamide gel in TG buffer. Because of the lower specific activity of the adenovirus L3 substrate in this experiment, it was necessary to expose lanes 3 and 4 to X-ray film five times longer than lanes 1 and 2 to obtain the same autoradiographic density. The positions of the complex (C) and RNP are indicated.

gels. Precursors containing a polyadenylation signal entered a different complex whose mobility was further retarded.

We believe that this complex is a site of cleavage and possibly polyadenylation for the following reasons. (i) The conditions required for complex formation (presence of a polyadenylation signal, incubation at 30°C, and presence of ATP or an ATP analog) were the same as those required for 3′-end processing. (ii) Both 3′-end processing and complex formation occurred without a lag period. (iii) The appearance and disappearance of the complex coincided with the initiation and cessation of processing. (iv) Processing and formation of a complex containing ^{32}P-labeled substrate could be prevented by excess ^{35}S-labeled homologous *tk* substrate or with heterologous precursor RNA containing the adenovirus L3 polyadenylation signal region.

Competition experiments were also conducted with RNAs which lacked various portions of the *tk* polyadenylation signal region. As expected, an RNA which lacks the entire *tk* polyadenylation signal region was unable to compete for complex formation or processing. No competition was seen with RNAs containing the GU cluster but lacking both AAUAAAs or with a substrate containing both AAUAAAs but lacking the GU cluster.

The lower level of complex detected with the adenovirus L3 precursor, an excellent substrate, requires an explanation. Adenovirus L3 precursor RNA was processed considerably more rapidly than *tk* substrate, and therefore there may be less L3 precursor RNA in complex form at any given time.

Hashimoto and Steitz (22) identified a complex immunoprecipitated by anti-Sm antibody; that complex protected the polyadenylation signal region of adenovirus L3 and E2A and SV40 early and late pre-mRNA substrates from RNase digestion. In all cases, the AAUAAA region was included in the portion of the substrate protected. Interestingly, in the case of the SV40 early substrate, only the second of two AAUAAAs was protected. Experiments in vivo with SV40 mutants indicate that only the second of the two AAUAAAs is part of the 3′-end RNA processing signal for the SV40 early transcription unit. Thus, the complex immunoprecipitated by antibody includes AAUAAA, but AAUAAA alone is not a sufficient signal for complex formation.

In another study, Zarkower and Wickens (46) identified a complex active in 3′-end RNA processing. Their assay involved use of an oligodeoxyribonucleotide complementary to the AAUAAA region of an SV40 late pre-mRNA substrate. When a complex was formed with the substrate, the oligonucleotide was unable to form an RNA-DNA hybrid and the RNA substrate was thus protected from cleavage by RNase H present in the nuclear extract. This complex, like the one we characterized, forms rapidly and requires a functional polyadenylation signal and ATP or an analog. A complex also formed on precleaved RNAs, containing AAUAAA but lacking the downstream GU cluster.

This complex may be involved only in polyadenylation and not in cleavage. The substrate requirements for that complex are an AAUAAA and a nearby 3′ terminus. Such RNAs are excellent substrates for polyadenylation in vitro and after microinjection into *Xenopus* germinal vesicles, and it is likely that these substrates would form a complex containing the AAUAAA and poly(A) polymerase. There is no requirement for the downstream second element. However, precleaved RNA was able to prevent processing of uncleaved substrate, indicating that components able to interact with precleaved RNAs are essential for cleavage and polyadenylation of precursor RNAs. Overall, this suggests that the same complex may be involved in both cleavage and at least the initial stages of polyadenylation.

Zarkower and Wickens noted that a complex formed with SV40 late precursor RNA was stabilized if 3′ dATP was used in place of ATP. We found (Fig. 8) that, in the presence of ATP analogs, the amount of complex formed was equal to or greater than that formed with ATP and that the complex did not disappear within 2 h. We also found the complex persisting when AMP(CH_2)PP and AMPP(CH_2)P were used in place of ATP. This contrasts with the finding that the complex described by Zarkower and Wickens (46) was stabilized by a 3′-terminal cordycepin residue but not by AMP(CH_2)PP.

The data we have presented and those described by others (22, 40, 46) suggest the following model for 3′-end RNA processing. (i) 3′-end RNA processing occurs in a complex which is formed between substrate RNAs and other components only if the substrate contains a poly(A) signal, if ATP or an analog is present, and if components are incubated at 30°C. (ii) Although AAUAAA alone may be sufficient for interaction of RNAs with processing components (46), a downstream GU cluster is required for formation of a complex which can be detected by gel mobility shift analysis. (iii) Cleavage occurs within the complex, and the subsequent association of the 5′ and 3′ half molecules with complex components is considerably weaker than the asso-

ciation of precursor RNA. (iv) Polyadenylation may occur after release of a 5′ half molecule from the complex, or polyadenylated 5′ half molecules are more weakly associated with the complex than is precursor.

We do not yet know the identity of the components of the processing complex. That snRNPs are involved in these reactions is suggested by the finding that anti-Sm antibodies prevent cleavage of precursor RNAs. The work of Hashimoto and Steitz (22) also suggests that complexes contain snRNPs, although snRNPs involved in 3′-end processing have not been identified. We expect an endonuclease to be a component. Poly(A) polymerase may be a component, or it may interact with precursor RNA only after endonucleolytic cleavage. Further understanding of the enzymology and mechanisms of 3′-end RNA processing will require purification of the components involved.

ACKNOWLEDGMENTS

We thank the members of our laboratory for valuable discussions and suggestions, Roger Denome for critical reading of the manuscript, and Mita Vogel for excellent technical assistance.

This research was supported by Public Health Service grant GM-33998 from the National Institutes of Health.

LITERATURE CITED

1. **Berget, S. M., and B. L. Robberson.** 1986. U1, U2, and U4/U6 small nuclear ribonucleoproteins are required for in vitro splicing but not for polyadenylation. Cell **46**:691–696.
2. **Birnboim, H. C., and J. Doly.** 1979. A rapid alkaline extraction procedure for screening recombinant plasmid DNA. Nucleic Acids Res. **7**:1413–1423.
3. **Birnstiel, M. L., M. Busslinger, and K. Strub.** 1985. Transcription termination and 3′ processing: the end is in site! Cell **41**:349–359.
4. **Black, D. L., and J. A. Steitz.** 1986. Pre-mRNA splicing in vitro requires intact U4/U6 small nuclear ribonucleoprotein. Cell **46**:697–704.
5. **Brody, E., and J. Abelson.** 1985. The "spliceosome": yeast pre-messenger RNA associated with a 40S complex in a splicing-dependent reaction. Science **230**:1344–1349.
6. **Carthew, R. W., L. A. Chodosh, and P. A. Sharp.** 1985. An RNA polymerase II transcription factor binds to an upstream element in the adenovirus major late promoter. Cell **43**:439–448.
7. **Clewell, D. B., and D. R. Helinski.** 1970. A membrane filter technique for the detection of complementary DNA. Biochemistry **9**:4428–4440.
8. **Cole, C. N., and G. M. Santangelo.** 1983. Analysis in Cos-1 cells of processing and polyadenylation signals by using derivatives of the herpes simplex virus type 1 thymidine kinase gene. Mol. Cell. Biol. **3**:267–279.
9. **Cole, C. N., and T. P. Stacy.** 1985. Identification of sequences in the herpes simplex virus thymidine kinase gene required for efficient processing and polyadenylation. Mol. Cell. Biol. **5**:2104–2113.
10. **Conway, L., and M. Wickens.** 1985. A sequence downstream of A-A-U-A-A-A is required for formation of simian virus 40 late mRNA 3′ termini in frog oocytes. Proc. Natl. Acad. Sci. USA **82**:3949–3953.
11. **Davanloo, P., A. H. Rosenberg, J. J. Dunn, and F. W. Studier.** 1984. Cloning and expression of the gene for bacteriophage T7 RNA polymerase. Proc. Natl. Acad. Sci. USA **81**:2035–2039.
12. **Dignam, J. D., R. M. Lebovitz, and R. G. Roeder.** 1983. Accurate transcription initiation by RNA polymerase II in a soluble extract from isolated mammalian nuclei. Nucleic Acids Res. **11**:1475–1489.
13. **Fitzgerald, M., and T. Shenk.** 1981. The sequence 5′-AAUAAA-3′ forms part of the recognition site for polyadenylation of late SV40 mRNAs. Cell **24**:251–260.
14. **Frendewey, D., and W. Keller.** 1985. Stepwise assembly of a pre-mRNA splicing complex requires U-snRNPs and specific intron sequences. Cell **42**:355–367.
15. **Fried, M., and D. M. Crothers.** 1981. Equilibria and kinetics of *lac* repressor-operator interactions by polyacrylamide gel electrophoresis. Nucleic Acids. Res. **9**:6505–6525.
16. **Gil, A., and N. J. Proudfoot.** 1984. A sequence downstream of AAUAAA is required for rabbit beta-globin mRNA 3′-end formation. Nature (London) **312**:473–474.
17. **Grabowski, P. J., R. A. Padgett, and P. A. Sharp.** 1984. Messenger RNA splicing in vitro: an excised intervening sequence and a potential intermediate. Cell **37**:415–427.
18. **Grabowski, P. J., S. R. Seiler, and P. A. Sharp.** 1985. A multicomponent complex is involved in the splicing of messenger RNA precursors. Cell **42**:345–353.
19. **Grabowski, P. J., and P. A. Sharp.** 1986. Affinity chromatography of splicing complexes: U2, U5, and U4+U6 small nuclear ribonucleoprotein particles in the spliceosome. Science **233**:1294–1299.
20. **Hart, R. P., M. A. McDevitt, H. Ali, and J. R. Nevins.** 1985. Definition of essential sequences and functional equivalence of elements downstream of the adenovirus E2A and the early simian virus 40 polyadenylation sites. Mol. Cell. Biol. **5**:2975–2983.
21. **Hart, R. P., M. A. McDevitt, and J. R. Nevins.** 1985. Poly(A) site cleavage in a HeLa nuclear extract is dependent on downstream sequences. Cell **43**:677–683.
22. **Hashimoto, C., and J. A. Steitz.** 1986. A small nuclear ribonucleoprotein associates with the AAUAAA polyadenylation signal in vitro. Cell **45**:581–591.
23. **Konarska, M. M., and P. A. Sharp.** 1986. Electrophoretic separation of complexes involved in splicing of precursors to mRNAs. Cell **46**:845–855.
24. **Krainer, A. R., and T. Maniatis.** 1985. Multiple factors including the small nuclear ribonucleoproteins U1 and U2 are necessary for pre-mRNA splicing in vitro. Cell **42**:725–736.
25. **Kramer, A., W. Keller, B. Appel, and R. Luhrmann.** 1984. The 5′ terminus of the RNA moiety of U1 small nuclear ribonucleoprotein particles is required for the splicing of messenger RNA precursors. Cell **38**:299–307.
26. **Leff, S. E., M. G. Rosenfeld, and R. M. Evans.** 1986. Complex transcriptional units: diversity in gene expression by alternative RNA processing. Annu. Rev. Biochem. **55**:1091–1117.
27. **McDevitt, M. A., M. J. Imperiale, H. Ali, and J. R. Nevins.** 1984. Requirement for a downstream sequence for generation of a poly(A) addition site. Cell **37**:993–999.
28. **McLauchlan, J., D. Gaffney, J. L. Whitton, and J. B. Clements.** 1985. The consensus sequence YGTGTTYY located downstream from the AATAAA signal is required for efficient formation of mRNA 3′ termini. Nucleic Acids Res. **13**:1347–1368.
29. **Mandel, M., and A. Higa.** 1970. Calcium-dependent bacteriophage DNA interaction. J. Mol. Biol. **53**:159–162.
30. **Manley, J. L., H. Yu, and L. Ryner.** 1985. RNA sequence containing hexanucleotide AAUAAA directs efficient mRNA polyadenylation in vitro. Mol. Cell. Biol. **5**:373–379.
31. **Moore, C. L., and P. A. Sharp.** 1984. Site-specific polyadenylation in a cell-free reaction. Cell **36**:581–591.
32. **Moore, C. L., and P. A. Sharp.** 1985. Accurate cleavage and polyadenylation of exogenous RNA substrate. Cell **41**:845–855.
33. **Moore, C. L., H. Skolnik-David, and P. A. Sharp.** 1985. Analysis of RNA cleavage at the adenovirus-2 L3 polyadenylation site. EMBO J. **5**:1929–1938.
34. **Nevins, J. R.** 1983. The pathway of eukaryotic mRNA formation. Annu. Rev. Biochem. **52**:441–466.
35. **Nevins, J. R., and J. E. Darnell.** 1978. Steps in the processing of Ad-2 mRNA: poly(A)$^+$ nuclear sequences are conserved and poly(A) addition precedes splicing. Cell **15**:1477–1493.
36. **Nevins, J. R., and M. C. Wilson.** 1981. Regulation of adenovirus-2 gene expression at the level of transcription termination and RNA processing. Nature (London) **290**:113–119.
37. **Padgett, R. A., S. M. Mount, J. A. Steitz, and P. A. Sharp.** 1983. Splicing of messenger RNA precursor is inhibited by antisera to small nuclear ribonucleoprotein. Cell **35**:101–107.
38. **Perkins, K. K., H. M. Furneaux, and J. Hurwitz.** 1986. RNA splicing products formed with isolated fractions from HeLa cells

are associated with fast-sedimenting complexes. Proc. Natl. Acad. Sci. USA **83**:887–891.

39. **Proudfoot, N. J., and G. G. Brownlee.** 1976. 3′ non-coding region sequences in eukaryotic messenger RNA. Nature (London) **263**:211–214.
40. **Ryner, L. C., and J. L. Manley.** 1987. Requirements for accurate and efficient mRNA 3′ end cleavage and polyadenylation of a simian virus 40 early pre-RNA in vitro. Mol. Cell. Biol. **7**:495–503.
41. **Sadofsky, M., and J. C. Alwine.** 1984. Sequences on the 3′ side of hexanucleotide AAUAAA affect efficiency of cleavage at the polyadenylation site. Mol. Cell. Biol. **4**:1460–1468.
42. **Sen, R., and D. Baltimore.** 1986. Inducibility of immunoglobulin enhancer-binding protein NF-kB by a posttranslational mechanism. Cell **47**:921–928.
43. **Singh, H., R. Sen, D. Baltimore, and P. A. Sharp.** 1986. A nuclear factor that binds to a conserved sequence motif in transcriptional control elements of immunoglobulin genes. Nature (London) **319**:154–158.
44. **Sperry, A. O., and S. M. Berget.** 1986. In vitro cleavage of the simian virus 40 early polyadenylation site adjacent to a required downstream TG sequence. Mol. Cell. Biol. **6**:4734–4741.
45. **Zarkower, D., P. Stephenson, M. Sheets, and M. Wickens.** 1986. The AAUAAA sequence is required both for cleavage and for polyadenylation of simian virus 40 pre-mRNA in vitro. Mol. Cell. Biol. **6**:2317–2323.
46. **Zarkower, D., and M. Wickens.** 1987. Formation of mRNA 3′ termini: stability and dissociation of a complex involving the AAUAAA sequence. EMBO J. **6**:177–186.
47. **Zhang, F., R. M. Denome, and C. N. Cole.** 1986. Fine-structure analysis of the processing and polyadenylation region of the herpes simplex virus type 1 thymidine kinase gene by using linker scanning, internal deletion, and insertion mutations. Mol. Cell. Biol. **6**:4611–4623.